

Impact of Meteorological Parameters on Atmospheric Turbidity over Lumbini, Nepal

Prakash M. Shrestha^{1,2}, Suresh P. Gupta^{1,*}, Usha Joshi¹, Krishna B. Rai¹, Narayan P. Chapagain³, Indra B. Karki¹, Khem N. Poudyal⁴

¹ Department of Physics, Patan Multiple Campus, TU

² Central Department of Physics (CDP), TU

³ Department of Physics, Amrit Campus, TU

⁴ Department of Applied Sciences and Chemical Engineering, Pulchowk Campus, TU

* Corresponding e-mail: suresh.gupta@pmc.tu.edu.np

Doi: <https://doi.org/10.3126/ppj.v3i2.66166>

Abstract

The main objective of this research is to study of impact of meteorological parameters on atmospheric turbidity index on Lumbini (27.49° N, 83.28° E, 110 m asl), Nepal for a period of one year (2018). The ground based data of spectral aerosol optical depth (AOD) are derived from Aerosol Robotic Network (AERONET) of NASA. Satellite based data of meteorological parameter (maximum temperature, minimum temperature, dew point, relative humidity, water content and rainfall) are downloaded from NASA website. Daily, monthly and seasonal variation of atmospheric turbidity is analyzed. The annual average of Angstrom exponential (α), Angstrom coefficient of turbidity (β) and Linke turbidity factor (L_T) are found 1.0 ± 0.2 , 0.36 ± 0.20 and 8.3 ± 2.5 respectively. Correlation coefficient of meteorological parameters with atmospheric turbidity is analyzed. No significant effect of maximum temperature, minimum temperature, dew point and water content on atmospheric turbidity. There is positive effect of rainfall on α , but negative effects of relative humidity and rainfall on β and L_T . Atmospheric turbidity index is an important for the air pollution. Result of this research work is beneficial for the further identification, impact and analysis of atmospheric turbidity index on meteorological parameters at different places with same geographical condition.

Keywords: Angstrom exponential, Angstrom coefficient of turbidity, Linke turbidity factor, meteorological parameter.

1. Introduction

The Sun radiates 4×10^{26} W energy [1]. About 1367 W of the solar energy incidents on one square meter area of the atmosphere when the Sun and the Earth are at 1 AU distance. Solar energy is a clean, renewable and sustainable energy for solar energy applications around the world [2]. Accurate estimation of solar radiation at given locations are required for radiation conversion device and photovoltaic cells [3]. The utilization of solar energy is a promising outlook for energy crisis and climate change. Many engineers, energy experts, policymakers and climate advocates have paid great attentions to the utilization of solar energy [4], which

has been applied to our lives, such as the design for agriculture, water resources and passive heating of buildings. The adoption of solar technologies is growing quickly [5]. The quality and amount of solar radiation passing through the atmosphere is altered by atoms molecules like ozone, water vapor, carbon dioxide as well as by liquid and solid aerosols that are present along the propagation path. Solar radiation is usually influenced by three groups of dynamic factors: Sun- Earth position, terrain, and atmospheric effects. Solar irradiance at ground level is highly dependent on the Earth's atmospheric turbidity [6]. Atmospheric Turbidity is a dimensionless measure of the opacity of a vertical column of the atmosphere. Both natural and anthropogenic aerosols influence on attenuation of solar energy [7]. Anthropogenic aerosols, black carbon are emitted by vehicles and kilns produces greenhouse effect. Black carbon melts ice on mountain. Particular matter (such as PM1.0, PM2.5, PM10) are responsible for respiratory illness. Atmospheric transparency can be affected both by natural phenomena within the Earth's atmosphere like clouds, dust, etc. and by human activity like factories, cars and many more. These atmospheric turbidity factors have been widely used at several places around the world based on solar irradiance measurements to quantify the effects of aerosols and air pollutants on degrading horizontal visibility and reducing the amount of solar radiation reaching the ground. The Linke turbidity factor have been studied by Cucumo et al.[8] at two locations in Italy and several other studies the Linke turbidity factor like Chile [9], and in Brazil [10]. The correlation between atmospheric turbidity and the local weather conditions shows that this increase is essentially due to the heavy water vapor content of maritime air masses, carried by the north-eastern winds prevalent during the afternoon [11]. This article deals with e deals with the estimation of atmospheric turbidity index. Solar irradiance is attenuated exclusively by perpetual atmospheric constituents under a clear and dry atmosphere. Atmospheric turbidity is function of optical depth. In recent decades, the estimate atmosphere turbidity index have been calculated based on spectral irradiance data [12]. In this research, we studied the impact of meteorological parameters on atmospheric turbidity over Lumbini, Nepal.

Nepal (26°22' N to 30°27' N and longitude of 80°04' E to 88°12' E) is situated at the complex terrain of the Trans-Himalaya region and is landlocked between India and China. It is about 800 km long and 200 km wide with an area of 147,516 km². Ecologically, Nepal is divided into three regions: Low-land, Mid-land, and High-land [13]. The elevation of the country ranges from 60 m to 8848 m above sea level. In this vast variation of its altitude, there is range from sub - tropical to Arctic region which is unique and complex climatic zone in the world [14]. Lumbini (27.49° N, 83.28° E, 110 m asl) is a Buddhist pilgrimage site in the Rupandehi District of Lumbini Province in Nepal. It is birthplace of Siddhartha Gautama (Budhha) at around 563 BCE. Lumbini has a number of older temples including the Mayadevi Temple and Ashok Stambha. Lumbini was made a World Heritage Site by UNESCO in 1997. The maximum and minimum temperature of Lumbini are 31.8°C and 18.7° C respectively. Annual rainfall is 1369.5 mm [15]. Area of Rupandehi district is 1,360 square km. The population and population density of the district are 880,196 and 647 per square km respectively in 2011 national census [16].

2. Materials and Methods

The solar energy is ultimate sources of all kinds of energy on the Earth through the atmosphere. Some part of radiated energy gets diffused, scattered, and absorbed by water droplets, gas molecules and aerosols [17]. Factors influencing a correct estimation of the incoming solar radiation include atmospheric conditions (e.g. air turbidity, cloudiness, aerosol, water vapor) and topography (e.g. shadowing by hills, mountains, nearby buildings, vegetation, etc.) [5]. Therefore, global solar radiation reaching to the earth is reduced due to atmospheric turbidity. In developing countries like Nepal, most of energy consumption is from wood, agriculture residue, cow dung, coal. It means that rest of energy is conventional energy. So, it emits huge amount of carbon dioxide and other harmful gases such as nitrous oxide, methane, carbon mono oxide etc. Study of atmospheric turbidity and its impact on solar radiation is essential for agriculture, Hydrology, climate change and energy harvesting [18]. In this study, the comparative influences of atmospheric air pollutant concentrations and meteorological parameters on atmospheric visibility, clearness index and turbidity were investigated. The critical relationship between atmospheric visibility, turbidity values and atmospheric air pollutants could be determined under different meteorological parameters. Figure 1 depict the map of Lumbini.

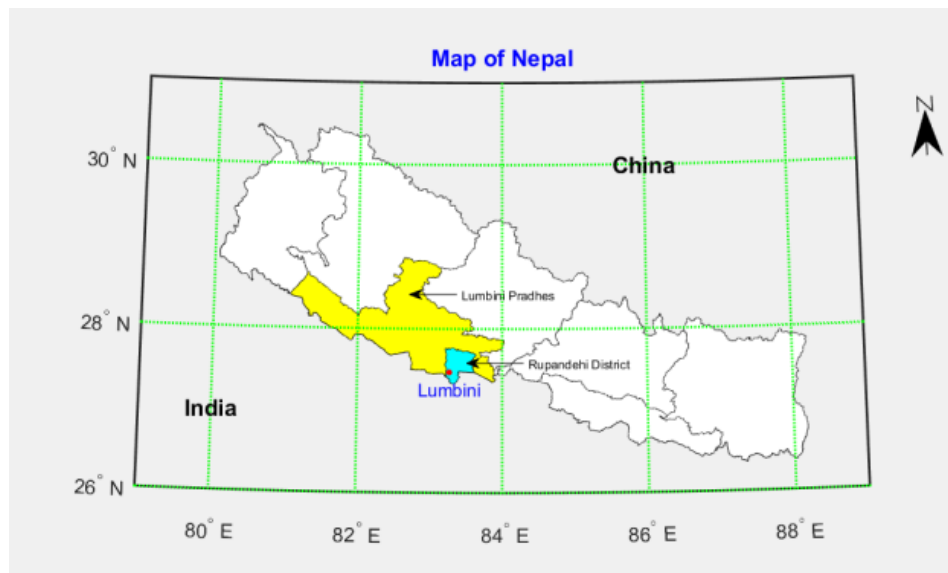


Figure 1: Map of Lumbini [source: Department of survey, Gov. of Nepal, 2020]

The solar energy passing through the atmosphere is scattered and absorbed by the atmosphere due to interacts with components like aerosol, cloud etc. According to Beer Lambert's law, the solar energy decreases exponentially in the atmosphere [19]. The attenuation of solar energy through a real atmosphere verse that through a clean, dry atmosphere gives atmospheric turbidity. There are large number of atmospheric turbidity factors. Angstrom turbidity coefficient (β), Angstrom exponential (α) and Linke turbidity factor (L_T) are mostly used [20]. According to angstrom model [21]

$$AOD = \beta \lambda^{-\alpha} \tag{1}$$

Here λ is wavelength. Angstrom exponent (α) is an important indicator of the foremost aerosol size [22]. α greater than two indicates small particles associated with combustion byproducts, and values less than one indicates large particles like sea salt and dust.

Linke (1922) proposed to express the total optical thickness of a cloudless atmosphere as the product of two terms, the optical thickness of water and aerosol free atmosphere and the Linke turbidity factor (L_T) [23]. According to Dogniaux,1974, Linke turbidity factor is [24]

$$L_T = \left(\frac{85+\gamma}{39.5e^{-\omega}+47.4} + 0.1 \right) (16 + 0.22w) \beta \tag{2}$$

Here γ is solar height ($90 - \theta_z$) and w is water content in cm. Solar zenith angle (θ_z) depends on solar declination (δ), latitude(ϕ) of the place , solar hour angle (ω) and day number of year (n_d) [25].

$$\theta_z = \cos^{-1}(\sin\delta \sin\phi + \cos\delta \cos\phi \cos\omega)$$

$$\delta = 23.45 \sin\left(\frac{360}{365}(284 + n_d)\right)$$

Daily ground based data of spectral aerosol optical depth (AOD) are collected from AERONET for Lumbini on 2018 of wavelength 675, 500, 440, 380 and 340 nm. Satellite based daily data of meteorological parameters (maximum temperature, minimum temperature, dew point, relative humidity water content and rainfall) are downloaded from NASA website. Open source software Python 3.7 is used to analysis and to plot graph. The quartiles (Q_1, Q_2, Q_3), skewness (γ_1) and kurtosis (γ_2) are used to analyzed nature of distribution of data [26]. Standard error (SE) is used as error bar in graph. Data presented in forms of 'mean (\bar{x}) standard deviation (σ)'.

$$SE = \frac{\sigma}{\sqrt{n}} \tag{3}$$

Here n is number of data. Correlation coefficient (r) is used to find relation between two data x and y . Its value range from -1 to +1.

$$r = \frac{\sum_{i=1}^n (x_i - \bar{x})(y_i - \bar{y})}{\sqrt{\sum_{i=1}^n (x_i - \bar{x})^2} \sqrt{\sum_{i=1}^n (y_i - \bar{y})^2}} \tag{4}$$

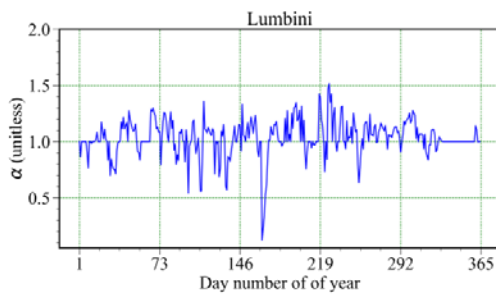
3. Results and Discussion

Daily data of spectral aerosol optical depth (AOD) for wavelength 675, 500, 440, 380 and 340-nm are downloaded from AERONET website for Lumbini on 2018. By using and aerosol optical depth (AOD), daily data of Angstrom exponential (α) and Angstrom coefficient of turbidity (β) are calculated by linear regression method for equation (1). Daily data of Linke turbidity factor (L_T) is calculated by using equation (2). Correlation coefficient (r) of meteorological parameter with atmospheric turbidity is calculated by using equation (4).

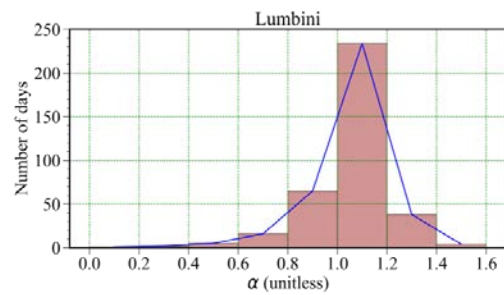
3.1 Variation of Atmospheric turbidity

3.1.1 Variation of Angstrom exponential (α)

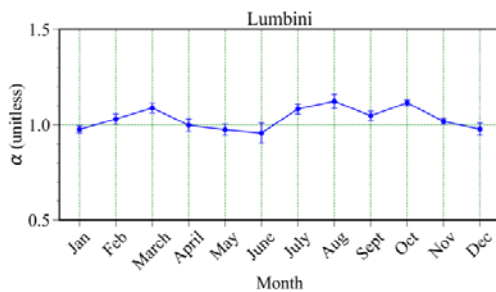
Figure 2(a) indicates daily variation of Angstrom exponential (α). During one year (2018) period, the greatest value of α is found 1.5 on August 15. As α is more than one, atmosphere of that day contains fine aerosol. The lower value of α is 0.1 on June 15. As α is smaller than one, atmosphere of that day contains coarse mode aerosol. The annual mean and standard deviation are found 1.0 and 0.2 respectively. Figure 2(b) shows histogram of α . The first quartile (Q_1), median (Q_2) and third quartile (Q_3) are observed 1.01, 1.0 and 1.1 individually. The skewness (γ_1) and the kurtosis (γ_2) are observed as -1.17 and 5.00 respectively. The distribution of α is negatively tailed and is not symmetric. Out of 365 study days, 224 days has α in between 1.0 to 1.2. Figure 2(c) shows monthly variation of α . The largest and smallest value of monthly average of α is calculated as 1.1 ± 0.2 in August and 0.9 ± 0.3 in June respectively. Variation of α is greater in March due to large standard deviation and is less in January due to small standard deviation. Figure 2(d) shows seasonal variation of α . The largest and smallest value of α is found 1.1 ± 0.1 in autumn and 0.9 ± 0.1 in winter respectively. Variation of α is greater in summer due to large standard deviation and is less in winter due to small standard deviation



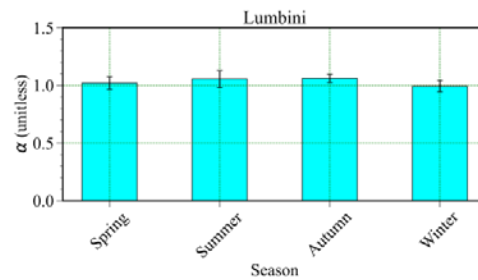
a) Daily variation



b) Histogram



c) Monthly variation

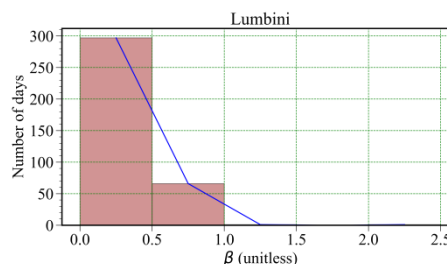
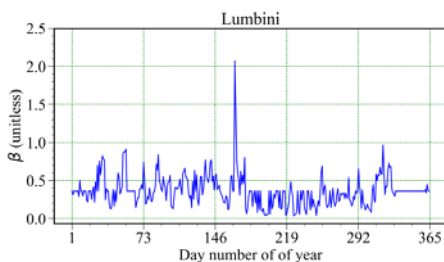


d) Seasonal variation

Figure.2: Variation of Angstrom exponential (α)

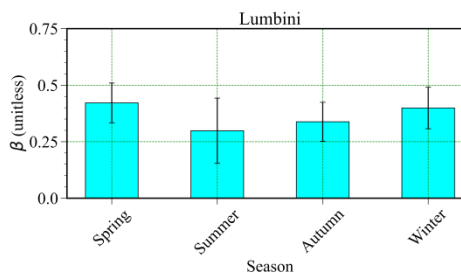
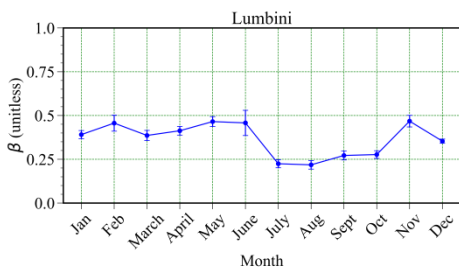
3.1.2 Variation of Angstrom turbidity coefficient (β)

Figure 3(a) indicates daily variation of Angstrom turbidity coefficient (β). During study period, the greatest value of β is found 2.07 on June 15, atmosphere of that day very turbid. The smallest value of β is 0.04 on August 16, atmosphere of that day is clear. The annual mean and standard deviation are calculated as 0.36 and 0.20 respectively. Figure 3(b) indicated histogram of β . The first quartile, second quartile and third quartile are calculated as 0.25, 0.36 and 0.42 respectively. The skewness and kurtosis are calculated as 2.28 and 13.98 respectively. The distribution of β is positively tailed and is not symmetric. Out of 365 study days, 297 days has β in between 0 to 0.5. Figure 3(c) indicates monthly variation of β . The largest and smallest value of monthly average of β is observed as 0.47 ± 0.18 in November and smaller 0.22 ± 0.14 in August respectively. Variation of β is large in March due to large standard deviation and is smaller in July due to small standard deviation. Figure 3(d) shows seasonal variation of β . During study period of one year 2018, the greatest and smallest value of average of β is calculated as 0.40 ± 0.16 in winter and 0.30 ± 0.25 in summer respectively. Variation of β is greater in spring due to large standard deviation and is smaller in summer due to small standard deviation.



a) Daily variation

b) Histogram



c) Monthly variation

d) Seasonal variation

Figure.3: Variation of Angstrom coefficient of turbidity (β)

In Kathmandu, Nepal on 1999, Angstrom turbidity coefficient was found 0.6247 ± 0.023 and 0.2997 ± 0.009 respectively [27]. In Jomsom (Nepal) in year 2012, the annual mean of Angstrom exponential and Angstrom turbidity coefficient were found 1.24 ± 0.54 and 0.05 ± 0.04 respectively [28]. On Bhaktapur (Nepal) in year 2013, the annual average of

Angstrom exponential, Angstrom turbidity coefficient was found 1.13 ± 0.21 and 0.18 ± 0.14 respectively [29].

3.1.3 Variation of Linke turbidity factor (L_T)

Figure 4(a) indicates daily variation of Linke turbidity factor (L_T). During study period, the greatest value of L_T is found 18.2 on June 15, atmosphere of that day highly polluted. The smaller value of L_T is 3.8 on September 5, atmosphere of that day is clear. The annual mean and standard deviation are calculated as 8.3 and 2.5 respectively. Figure 4(b) indicates histogram of L_T . The Q_1 , Q_2 and Q_3 are observed as 6.6, 8.4 and 9.2 respectively. The skewness and kurtosis are calculated as 0.77 and 0.02 respectively. The distribution of L_T is positively tailed and is not symmetric. Out of 365 study days, 198 days has L_T in between 8 to 12. Figure 4(c) indicates monthly variation of L_T . During study period of one year 2018, the greatest and lowest value of monthly average of L_T is found 9.5 ± 2.7 in November and 6.5 ± 1.7 in July respectively. Variation of L_T is greatest in March due to large standard deviation and is smaller in July due to small standard deviation. Figure 4(d) indicates seasonal variation of L_T . During study period, the largest and lowest value of average of L_T are observed as 9.3 ± 2.3 in spring and 7.3 ± 2.2 in summer respectively. Variation of L_T is large in spring due to the greatest value of standard deviation and is less in summer due to smallest value of standard deviation.

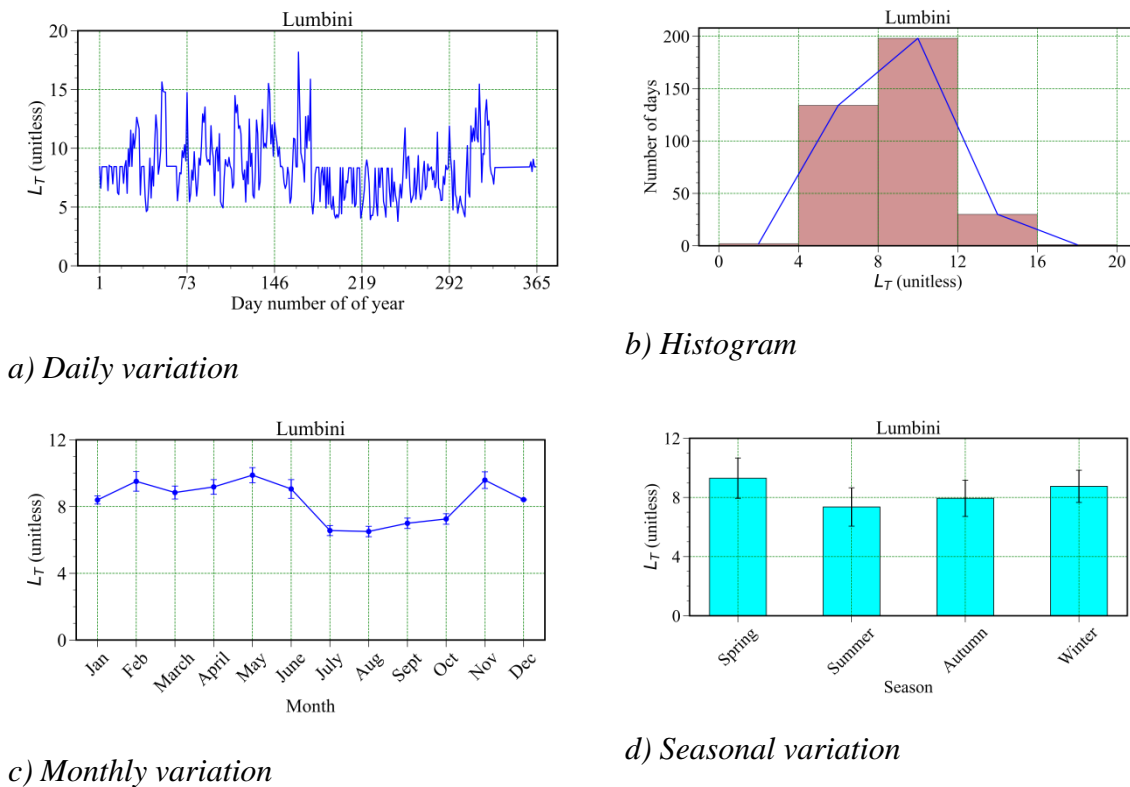
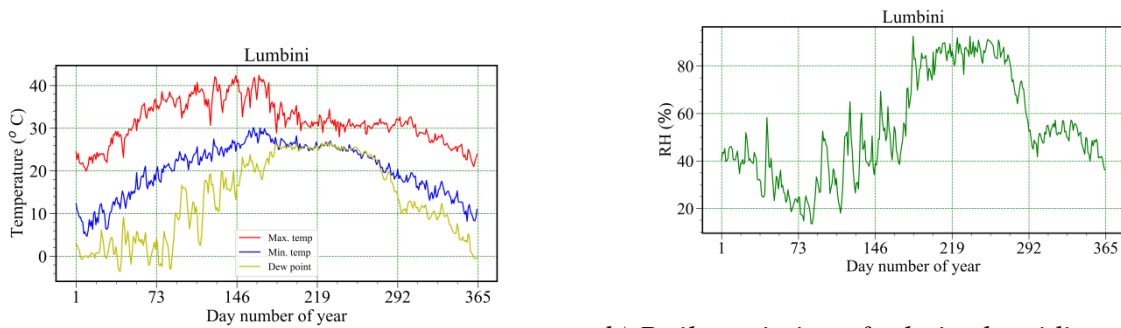


Figure.4: Variation of Linke turbidity factor (L_T)

In Wuhan (China) from 2010 to 2011, Linke turbidity is 3.3 to 7.7 [30]. In the period of 1993 to 2000 Linke turbidity are 7.5 in Kolkata, 4.6 in Poona, 6.4 in Jaipur and 6.8 in New Delhi of India [31]. On Deukhuri Valley of Dang (Nepal) in period of 2015 to 2018, the annual average value of Linke turbidity factor is found 2.5 ± 1.1 [32]. on Pokhara (Nepal) for 2017, the annual mean of Angstrom exponential, Angstrom coefficient of turbidity and Linke turbidity are found 2.5 ± 1.1 , 0.19 ± 0.17 and 6.7 ± 3.4 respectively [33].

3.2 Variation of meteorological parameters and Atmospheric turbidity

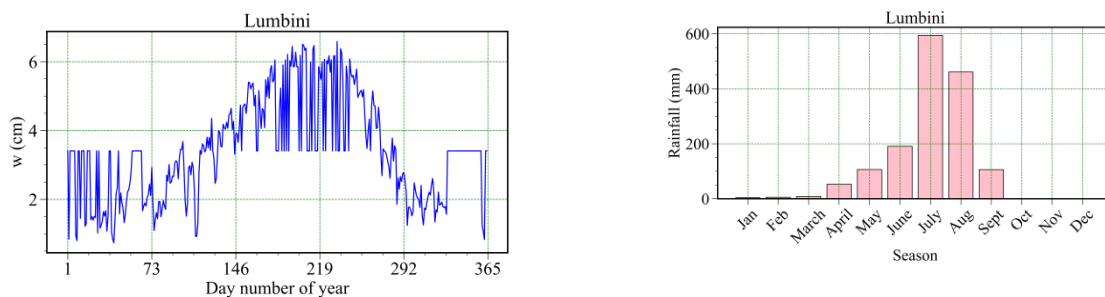
Figure 5(a) indicates daily variation of maximum temperature, minimum temperature and dew point. The highest value of maximum temperature is 42.4°C on June 16, hottest day of the year. The annual average is $31.6 \pm 5.2^\circ\text{C}$. Figure 6(a) shows correlation coefficient of atmospheric turbidity index with meteorological parameters. The correlation coefficient of maximum temperature with α , β and L_T are -0.03, 0.13 and 0.15 respectively. Those values are not significant. The lowest value of minimum temperature is 4.7°C on January 11, coldest day of the year. The annual average of minimum temperature is $20.2 \pm 6.2^\circ\text{C}$. The correlation coefficient of minimum temperature with α , β and L_T are 0.05, -0.09 and -0.09 respectively. Those values are not significant. The annual average of dew point is $13.5 \pm 9.5^\circ\text{C}$. The correlation coefficient of dew point with α , β and L_T are 0.08, -0.23 and -0.35 respectively. No significant effect of dew point on atmospheric turbidity index. Figure 5(b) shows daily variation of relative humidity (RH). The annual average of RH is $54 \pm 22\%$. The correlation coefficient of RH with α , β and L_T are 0.13, -0.34 and -0.36 respectively. No significant effect of RH on α , but negative affect on β and L_T . Figure 5(c) indicates daily variation of water content (w). The annual average of w is $3.4 \pm 1.7\text{ cm}$. The correlation coefficient of w with α , β and L_T are 0.08, -0.21 and -0.21 respectively. No significant effect of w on atmospheric turbidity index. Figure 5(d) shows monthly variation of rainfall. The annual rainfall is 1529.4 mm. The correlation coefficient of rainfall with α , β and L_T are 0.40, -0.63 and -0.64 respectively. There is positive effect of rainfall on α , but negative effect of rainfall on β and L_T .



a) Daily variation of maximum temperature, minimum

b) Daily variation of relative humidity

temperature and dew point



c) Daily variation of water content

d) Monthly variation of rainfall

Figure.5: Variation meteorological parameters

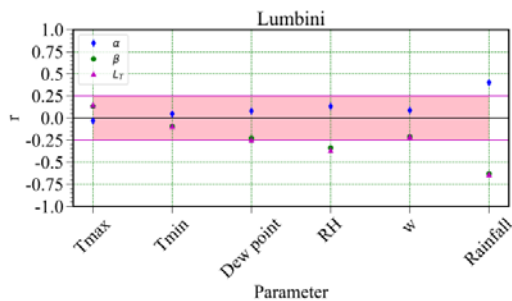


Figure.6: Correlation coefficient of meteorological parameters

4. Conclusion

In study period of one year (2018) on Lumbini (Nepal), the annual average of Angstrom exponential (α), Angstrom coefficient of turbidity (β) and Linke turbidity factor (L_T) are calculated as 1.0 ± 0.2 , 0.36 ± 0.20 and 8.3 ± 2.5 individually. The study of atmospheric

turbidity index has great significance to the detection of solar energy potential, global warming and climate change of the location. A comparison of observed values of turbidity parameter with other major cities of the world shows that Lumbini is polluted as compared to cities like Wuhan, New Delhi, Kolkota, Jaipur etc. Correlation coefficient of meteorological parameter with atmospheric turbidity are calculated and analyzed. No significant effect of maximum temperature, minimum temperature, dew point and water contains on atmospheric turbidity. There is positive effect of rainfall on α , but negative effects of relative humidity and rainfall on β and L_T .

Acknowledgment

The authors would like to thank the faculty members of the Institute of Science and Technology (IoST), the Central Department of Physics (CDP), and the Department of Physics of the Patan Multiple Campus. The NASA for data and the Nepal Academy of Science and Technology (NAST) for PhD fellowship are greatly appreciated by the authors. We would also like to thank the Association of Nepali Physicists in America (ANPA) and the Nepal Physical Society (NPS) for their assistance with the Python computer programming training.

References

- [1] Poudyal KN, Bhattarai BK, Sapkota B, Kjeldstad B. Solar radiation potential at four sites of Nepal (2011). *Journal of the Institute of Engineering*, **8**: 189–197.
- [2] Purohit I, Purohit P (2015). Inter-comparability of solar radiation databases in Indian context. *Renewable and Sustainable Energy Reviews*, **50**: 735–747.
- [3] Kambezidis H, Psiloglou B, Karagiannis D, Dumka U, Kaskaoutis D(2016). Recent improvements of the meteorological radiation model for solar irradiance estimates under all-sky conditions. *Renewable Energy*, **93**:142–158.
- [4] Solangi K, Islam M, Saidur R, Rahim N, Fayaz H(2011). A review on global solar energy policy. *Renewable and sustainable energy reviews*, **15**: 2149–2163.
- [5] Agugiaro G, Nex F, Remondino F, De Filippi R, Droghetti S, Furlanello C(2012). Solar radiation estimation on building roofs and web-based solar cadastre. *ISPRS Ann. Photogramm. Remote Sens. Spat. Inf. Sci*, **1**: 177–182.
- [6] Kosmopoulos PG, Kazadzis S, El-Askary H, Taylor M, Gkikas A, Proestakis E, et al(2018). Earth-observation-based estimation and forecasting of particulate matter impact on solar energy in Egypt. *Remote Sensing*, **10**: 1870.
- [7] Ramanathan V, Carmichael G. Global and regional climate changes due to black carbon (2008). *Nature Geoscience*, **1**: 221–227.
- [8] Cucumo M, Marinelli V, Oliveti G (1999). Data bank experimental data of the Linke turbidity factor and estimates of the Angstrom turbidity coefficient for two Italian localities. *Renewable energy*, **17**: 397–410.
- [9] Behar O, Sbarbaro D, Marzo A, Moran L (2019). A simplified methodology to estimate solar irradiance and atmospheric turbidity from ambient temperature and relative humidity. *Renewable and Sustainable Energy Reviews*, **116**: 109310.
- [10] Flores JL, Karam HA, Marques Filho EP, Pereira Filho AJ (2016). Estimation of atmospheric turbidity and surface radiative parameters using broadband clear sky solar irradiance models in Riode Janeiro Brasil. *Theoretical and applied climatology*, **123**: 593–617.

- [11] Chaabane M, Masmoudi M, Medhioub K (2004). Determination of Linke turbidity factor from solar radiation measurement in northern Tunisia. *Renewable Energy*, **29**: 2065–2076.
- [12] Flowers E, McCormick R, Kurfis K (1969). Atmospheric turbidity over the United States, 1961–1966. *Journal of Applied Meteorology and Climatology*, **8**: 955–962.
- [13] Joshi U, Shrestha P, Maharjan S, Bhattarai A, Bhattarai N, Chapagain N, et al(2022). Estimation of solar insolation and Angstrom– Prescott coefficients using sunshine hours over Nepal. *Advances in Meteorology*.
- [14] Majupuria T C MRK (1999). Nepal nature’s paradise: insight into diverse facets of topography, flora and Ecology, *M Devi, Gwalior, India*.
- [15] CBS (2012). Environment Statistics of Nepal, *Central Bureau of Statistics, National Planning Commission Secretariat, Government of Nepal*.
- [16] CBS (2011). National Population and Housing Census 2011, *Central Bureau of Statistics, National Planning Commission Secretariat, Government of Nepal*.
- [17] Poudyal KN, Bhattarai BK, Sapkota B, Kjeldstad B (2012). Estimation of global solar radiation using clearness index and cloud transmittance factor at trans-himalayan region in Nepal.
- [18] Poudyal KN, Bhattarai BK, Sapkota B, Kjeldstad B, Daponte P (2013). Estimation of the daily global solar radiation; Nepal experience. *Measurement*, **46**: 1807–1817.
- [19] Lothian G (1963). Beer’s law and its use in analysis. a review. *Analyst*, **88**: 678–685.
- [20] Eltbaakh YA, Ruslan MH, Alghoul M, Othman MY, Sopian K (2012). Issues concerning atmospheric turbidity indices. *Renewable and Sustainable Energy Reviews*, **16**: 6285–6294.
- [21] Angstrom A (1961). Techniques of determining the turbidity of the atmosphere. *Tellus*, **13**:214–223.
- [22] Schuster GL, Dubovik O, Holben BN (2006). Angstrom exponent and bimodal aerosol size distributions. *Journal of Geophysical Research: Atmospheres*,:111.
- [23] Ineichen P, Perez R (2002). A new air mass independent formulation for the Linke turbidity coefficient. *Solar Energy*, **73**:151–157.
- [24] Dogniaux R (1974). Representations analytiques descomposantes durayonnement lumineux solaire: conditions decielserein, *Institut royal meteorologique de Belgique*.
- [25] Iqbal M (1983). An introduction to solar radiation, *New York: Academic Press*.
- [26] Murray R Spiegel LJS (1998). Schaum’s Outline of Theory and Problems of Statistics (Schaum’s Outline Series), *McGraw-Hill*.
- [27] Sapkota B, Dhaubhadel R (2002). Atmospheric turbidity over Kathmandu valley. *Atmospheric Environment*, **36**:1249–1257.
- [28] Shrestha PM, Joshi U, Chapagain NP, Karki IB, Poudyal KN (2020). Study of variation of aerosols on high mountain, jomsom. *Molung Educational Frontier*, **10**: 147– 155.
- [29] Shrestha P, Chapagain N, Karki I, Poudyal K (2020). Study of linke turbidity factor over Bode, Bhaktapur. *Journal of Nepal Physical Society*, **6**: 66–73.
- [30] Wang L, Chen Y, Niu Y, Salazar GA, Gong W (2017). Analysis of atmospheric turbidity in clear skies at Wuhan, central China. *Journal of Earth Science*, **28**: 729–738.
- [31] Narain L, Garg S (2013). Estimation of linke turbidity factors for different regions of India. *International Journal of Environment and Waste Management*, **12**: 52–64.
- [32] Shrestha P, Gupta S, Joshi U, Chapagain N, Karki I, Poudyal K (2022). Atmospheric linke turbidity index over Deukhuri valley, Dang. *Journal of Nepal Physical Society*, **8**: 1–6.
- [33] Shrestha PM, Gupta SP, Joshi U, Chapagain NP, Karki IB, Poudyal KN (2023). Atmospheric turbidity index on Pokhara. *Patan Prospective Journal*, **3**: 162–172.